



DOX/IL-2/IFN- γ co-loaded thermo-sensitive polypeptide hydrogel for efficient melanoma treatment



Qiang Lv^{a, b}, Chaoliang He^{b, *}, Fenli Quan^b, Shuangjiang Yu^b, Xuesi Chen^b

^a Institute of Translational Medicine, The First Hospital of Jilin University, Changchun, 130021, China

^b Key Laboratory of Polymer Ecomaterials, Changchun Institute of Applied Chemistry, Chinese Academy of Sciences, Changchun, 130022, China

ARTICLE INFO

Article history:

Received 28 July 2017

Received in revised form

17 August 2017

Accepted 25 August 2017

Available online 6 September 2017

Keywords:

Polypeptide hydrogel

Sustained co-delivery

Combination therapy

Local cancer treatment

Thermosensitive hydrogel

ABSTRACT

Melanoma has been a serious threat to the human health; however, effective therapeutic methods of this cancer are still limited. Combined local therapy is a crucial approach for achieving a superior anti-tumor efficacy. In this paper, a chemo-immunotherapy system of DOX, IL-2 and IFN- γ based on poly(γ -ethyl-L-glutamate)-poly(ethylene glycol)-poly(γ -ethyl-L-glutamate) (PELG-PEG-PELG) hydrogel was developed for local treatment of melanoma xenograft. The drug release process of this system exhibited a short term of burst release (the first 3 days), followed by a long-term sustained release (the following 26 days). The hydrogel degraded completely within 3 weeks without obvious inflammatory responses in the subcutaneous layer of rats, showing a good biodegradability and biocompatibility. The DOX/IL-2/IFN- γ co-loaded hydrogel also showed enhanced anti-tumor effect against B16F10 cells *in vitro*, through increasing the ratio of cell apoptosis and G2/S phase cycle arrest. Moreover, the combined strategy presented improved therapy efficacy against B16F10 melanoma xenograft without obvious systemic side effects in a nude mice model, which was likely related to both the enhanced tumor cell apoptosis and the increased proliferation of the CD3⁺/CD4⁺ T-lymphocytes and CD3⁺/CD8⁺ T-lymphocytes. Overall, the strategy of localized co-delivery of DOX/IL-2/IFN- γ using the polypeptide hydrogel provided a promising approach for efficient melanoma therapy.

© 2017 The Authors. Production and hosting by Elsevier B.V. on behalf of KeAi Communications Co., Ltd. This is an open access article under the CC BY-NC-ND license (<http://creativecommons.org/licenses/by-nc-nd/4.0/>).

1. Introduction

Melanoma, one kind of highly aggressive cancer, has been a serious threat to the human health. It is estimated that about 80% of skin cancer due to the melanoma. The median survival of patients with distant metastases melanoma is no more than 1 year [1,2] and the 5-years survival is only 5–10% [3]. However, the incidence and the mortality of melanoma have been increasing over the past three decades estimated by the World Health Organization (WHO) [4]. The valid therapy for melanoma is urgently needed.

The common strategies for the cancer therapy are chemotherapy, radiotherapy and surgical treatment. However, the defects of chemotherapy, such as high frequency injection, rapid drug metabolism, low utilization of the drug and serious side effects severely influenced therapeutic effect. The radiotherapy and

surgical treatment may even do harm to the body. Recently, the immunotherapy, including cytokine therapy, immune-cell therapy and the targeted monoclonal antibody therapy, has been a promising strategy for the cancer therapy [5]. The cytokines including IL-2, IL-6, IL-12, IFN- α , IFN- β , IFN- γ [6] and TNF- α [7], the immune-cell including NK cells [8,9] and dendritic cells [10], as well as the monoclonal antibodies including ipilimumab and nivolumab [10,11], anti-cytotoxic T-lymphocyte-associated antigen 4 (anti-CTLA-4) antibodies, anti-programmed cell death protein 1 (anti-PD-1) antibodies [3] have been used for the cancer treatment. Up to now, the Food and Drug Administration (FDA) has approved a range of cytokines and antibodies such as IL-2, IFN- α , IFN- β and ipilimumab for the cancer immune treatment, which lights up a hope for efficient melanoma therapy.

To improve therapeutic efficacy of cancer, the combined treatment, localized treatment and targeted treatment have been developed. The combined therapy strategies including surgery/chemotherapy [12], chemotherapy/radiotherapy [13], multidrug chemotherapy [14], chemotherapy/immunotherapy [15], chemotherapy/gene therapy [16], chemo/hormonal therapy [17] and

* Corresponding author.

E-mail address: clhe@ciac.ac.cn (C. He).

Peer review under responsibility of KeAi Communications Co., Ltd.

immunotherapy/antiangiogenic [10] are the commonly combined styles for the cancer clinical treatment. DOX, an important chemotherapeutic agent acting by interacting with DNA double helices, presents wide anti-tumor activity such as lung, breast, melanoma, prostate and osteosarcoma cancer [18,19]. The combination of DOX with other therapeutic agent is usually be used for the cancer combined treatment, such as the combination of doxorubicin (DOX) with cisplatin (CDDP) for the bladder carcinoma and Meth-AR-1 tumor treatment [20], the combination of camptothecin (CPT), trastuzumab (TTZ), and DOX, which targeted at cell membrane, cytoplasm and nucleus of cancer cells, respectively, for a better inhibition of breast cancer cells [21], as well as the combination of DOX with TRAIL (membrane-associated tumor necrosis factor-related apoptosis-inducing ligand) for enhancing the MDA-MB-231 xenograft tumor therapeutic efficacy [22]. IL-2 and IFN- γ , the activated T-cell response cytokines that present encouraging anti-tumor activity [22,23] are also could be combined with other therapy agents to enhance the cancer therapy efficacy, such as the combination of IL-2 and TGF- β inhibitor [24], the combination of IL-2 and IFN- γ [25] and the combination of DOX, IL-2 and IFN- γ [26]. For the melanoma, combined therapies are often used to enhance the therapy efficacy, such as the combination of cisplatin, vinblastine, docarbazine, IL-2 and IFN- α [27], the combination of cisplatin, carmustine, dacarbazine and tamoxifen [28], the combination therapy of human mesenchymal stromal cells and doxorubicin [29], the combination of nivolumab and ipilimumab antibodies [29], the combination of IL-2 and IFN- γ [25], the combination of trabectedin and anti-PD-1 antibody [30] and the combination of cisplatin (CDDP)/recombinant rIL-2 and IFN- α [31,32].

The local therapy is another effective strategy to improve therapeutic efficacy of cancer, which has also been investigated for cancer immunotherapy [33]. Various drug delivery systems including iron oxide particles, polymeric particles, quantum dots, liposomes and thermo-sensitive hydrogels have been developed for the local therapy [34]. The thermo-sensitive hydrogels with the properties of easy to use, sustained drug release profile and reduced systemic toxicity of drugs have shown great potential for local cancer treatment. Qiao et al. [35] found the thermo-sensitive poly(lactic-co-glycolic acid)-poly(ethylene glycol)-poly(lactic-co-glycolic acid) triblock copolymer (PLGA-PEG-PLGA) hydrogel loaded with IL-2 showed encouraging anti-tumor effect as a promising platform for the immunotherapy of cancer. Moreover, the thermo-sensitive hydrogels could also be used as drug delivery systems for the combined therapy. For instance, based on poly(ϵ -caprolactone)-poly(ethylene glycol)-poly(ϵ -caprolactone) triblock copolymer (PCL-PEG-PCL) hydrogel, Peng et al. [36] developed a chemotherapy/radiotherapy combined system using liposomal doxorubicin and radionuclide (^{188}Re -Tin colloid) for the local therapy of hepatocellular carcinoma *in vivo*, which obtained 80% regression of tumor. In our previous studies, we [19] developed several chemotherapy/immunotherapy combined systems based on injectable hydrogels, which were used for localized and simultaneous delivering chemotherapeutic drugs (DOX and CDDP) and immunomodulating cytokines (IL-2, IFN- γ and IL-6), leading to obvious synergistic anti-tumor efficacy *in vitro* and *in vivo*. Among the injectable hydrogel systems, a kind of thermosensitive polypeptide hydrogels of poly(ethylene glycol)/poly(γ -ethyl-L-glutamate) (PEG/PELG) block copolymers have shown unique advantages including good biocompatibility, biodegradability, as well as convenient for drug loading and administration *in vivo* through a non-invasive procedure [37]. In addition, polypeptide hydrogels have the merits of lower critical gelation concentrations, no acid microenvironment after degradation, and non-covalent interactions with some bioactive molecules for sustained release and retaining the bioactivity, compared with other thermo-gelling

hydrogels, such as polyester-based hydrogels.

In this paper, we developed a chemo-immunotherapy system based on the thermosensitive PELG-PEG-PELG hydrogel co-loaded with DOX, IL-2 and IFN- γ for the therapy of melanoma xenograft nude mice model. Moreover, the biocompatibility, degradation, drug release behavior, and the toxicity mechanism of the DOX/IL-2/IFN- γ co-loaded hydrogel were also investigated in detail.

2. Experimental section

2.1. Materials

Poly (ethylene glycol) (mPEG₄₅, $M_n = 2000$) was obtained from Sigma-Aldrich (USA). L-glutamate was obtained from Huishi company (China). DOX·HCl was purchased from Beijing Huafeng United Technology Co., Ltd (China). IL-2 (3.0×10^7 IU mg^{-1}) was purchased from Amoytop Biotech (China). IFN- γ (5.0×10^7 IU mg^{-1}) was purchased from Nanjing GenScript (China) Co., Ltd. CD3/CD4/CD8/CD3e/CD49 antibodies were purchased from BioLegend (USA). The IL-2 and IFN- γ detection ELISA kits were purchased from Baijin Biotech Co., Ltd (China). The cell cycles detection kit and the cell apoptosis detection kit were purchased from KeyGEN BioTECH and BestBio BioTECH, respectively, (China). The trizol was obtained from Invitrogen (USA). The Prime Script™ RT reagent kit and the SYBR®Premix Ex Taq™ (Tli RNase H Plus) were obtained from TAKARA (Japan). The primers were synthesized by Sangon Biotech. (China). TUNEL assay kit was purchased from Roche (Switzerland). UltraSensitive™ SP IHC kit was purchased from Maixin Biotech Co., Ltd (China). The other materials were obtained as previous report [37].

2.2. Synthesis and characterization of PELG₇-PEG₄₅-PELG₇

The synthesis of PELG₇-PEG₄₅-PELG₇ copolymer was carried out *via* ring-opening polymerization of γ -ethyl-L-glutamate-*N*-carboxyanhydride (ELG-NCA) initiated by NH_2 -PEG- NH_2 as previous reported [37]. The resulting triblock copolymer was dissolved into TFA for ^1H NMR spectra analysis. Moreover, the molecular weights (MW) and the polydispersity (PDI) of the polymer were analyzed by gel permeation chromatography (GPC).

2.3. Rheology analysis and phase diagram

The rheology analysis of the PELG₇-PEG₄₅-PELG₇ solutions in phosphate buffer saline (PBS) at different concentrations was carried out on a Physica MCR 301 Rheometer (Anton Paar) at a heating rate of 0.5 °C per minute, a frequency of 1 Hz and a controlled strain of 1% as reported [37].

The sol-gel phase transition temperatures of the PELG₇-PEG₄₅-PELG₇ solutions with or without drugs were also measured as reported [37]. Briefly, the copolymer solutions or drug-containing copolymer solutions of different concentrations were stirred in vials at 0 °C for 1 day and then placed into a water bath environment with the temperature being increased steadily (2 °C per 10 min). The temperature was regarded as the sol-gel transition temperature when no flow was observed after inverting the vial for about 30 s.

2.4. Measurement of drug release *in vitro*

0.5 ml of the well dissolved PELG₇-PEG₄₅-PELG₇ copolymer solutions (4 wt%) containing drugs (DOX: 1.0 mg/ml, IL-2: 10 $\mu\text{g}/\text{ml}$, IFN- γ : 10 $\mu\text{g}/\text{ml}$) were introduced into the vials with an inner diameter of 16 mm, and then these copolymer solutions were allowed to form hydrogels by incubating at 37 °C for 10 min. After

that, 3 ml of release medium (PBS containing 0.1% SDS) was added into the vial as reported [35]. At pre-setting time intervals, 2 ml of the release medium was collected periodically and the same volume of fresh medium was re-added. DOX in the collected release medium was measured by fluorescence method and the released IL-2 and IFN- γ were measured using the ELISA kit. Briefly, the kit was balanced for 30 min in room temperature after being taken out from the environment at 4 °C. Then the released IL-2/IFN- γ sample was diluted for 5 times and standard was added into the wells. After being incubated for 2 h at 37 °C, the standard and samples were discarded and the plate was washed using wash buffer. Then the HRP-conjugate reagent was added, incubated for another 1 h at 37 °C and washed using wash buffer. After incubating with chromogen solutions A and B for 15 min at 37 °C, the stop solution was added and the OD_{450nm} values of wells were measured to calculate the concentrations of the released IL-2/IFN- γ sample.

2.5. *In vitro* biocompatibility of the PELG₇-PEG₄₅-PELG₇ copolymer

The cytocompatibility of the triblock copolymer was measured by methyl thiazolyl tetrazolium (MTT) against B16F10 cells. Briefly, the 96-well plates seeded with dulbecco's modified eagle medium (DMEM) containing cells (1×10^4 cells/well) were incubated at 37 °C and 5% of CO₂ for 24 h. Then the medium was changed for fresh medium and the copolymer solutions of different concentrations were added. The PBS and PEI treatments were used as negative and positive controls, respectively. After incubation for another 24 h, the copolymer solutions were discarded and the cells were washed with PBS and then subjected to MTT assays. The cell viability was calculated according to the following formula: Cell viability (%) = (OD_{Sam}/OD_{PBS}) × 100%, where OD_{Sam} and OD_{PBS} represent the absorbencies of the cells treated with polymer and PBS, respectively, by using a Bio-Rad 680 microplate reader at 490 nm.

2.6. Cytotoxicity measurement of DOX/IL-2/IFN- γ combination *in vitro*

The cytotoxicity of drugs was measured by MTT against B16F10 cells. Briefly, the 96-well plates seeded with DMEM containing cells (5000 cells/well) were incubated at 37 °C and 5% of CO₂ for 24 h. Then the medium was replaced with fresh medium containing drugs (DOX: 1 mg/ml, IL-2 and IFN- γ : 10 μ g/ml), followed by further incubating for 5 days. After that, the cell viability was measured by MTT and the cell viability was calculated according to the formula: Cell viability (%) = (OD_{drugs}/OD_{PBS}) × 100%, where OD_{drugs} and OD_{PBS} represent the absorbencies of the cells treated with drugs and PBS, respectively.

The cytotoxicities of the drug-loaded hydrogels were also measured by MTT as follows: the 24-well plates seeded with DMEM containing B16F10 cells (2.5×10^4 cells/well) were incubated at 37 °C and 5% of CO₂ for 24 h. Then the medium was discarded and 5 μ l of the copolymer solution incorporating drugs (DOX: 1 mg/ml, IL-2 and IFN- γ : 10 μ g/ml) was added into each well. After the hydrogel formed by incubating at 37 °C, fresh medium was added (0.5 ml per well) and incubated for 5 days. Then the cell viability was measured by MTT and the cell viability value was calculated according to the formula: Cell viability (%) = (OD_{Gel/drugs}/OD_{PBS}) × 100%, where OD_{Gel/drugs} and OD_{PBS} represent the absorbencies of the cells treated with drug-loaded hydrogel and PBS, respectively.

The experimental groups of DOX-loaded hydrogel group, IL-2/IFN- γ co-loaded hydrogel group and DOX/IL-2/IFN- γ co-loaded hydrogel group were abbreviated as G-DOX, G-IL-2/IFN- γ and G-DOX/IL-2/IFN- γ groups, respectively.

2.7. Analysis of cell apoptosis induced by drug-loaded hydrogel

The apoptosis of B16F10 cells after treating with the drug-loaded hydrogel was detected by flow cytometry. Briefly, the 6-well plates seeded with DMEM containing cells (3×10^5 cells/well) were incubated for 24 h at 37 °C. Then the medium was discarded and 5 μ l of the hydrogel precursor solutions incorporating drugs (DOX: 1 mg/ml, IL-2 and IFN- γ : 10 μ g/ml) was added into each well. After the hydrogel formed by incubating at 37 °C, fresh medium was added (2 ml per well) and incubated for 20 h. Then the cells were digested by trypsin, centrifuged at 3000 rpm for 5 min, and resuspended in binding buffer. After being stained using Annexin V-APC and 7-AAD for 15 min, the cells were subjected to the apoptosis analysis by FACS within 1 h.

Moreover, the expression of apoptosis-related genes in the treated B16F10 cells were also detected by quantitative real-time PCR (qRT-PCR) as described [16]. Briefly, B16F10 cells were seed in 6-well plates, followed by adding the drug-loaded hydrogels as above. After culture of 24 h, the cells were harvested and the RNA of the cells was extracted using trizol reagent to be reverse-transcribed cDNA using Prime Script™ RT reagent kit. Then qRT-PCR was carried out according to the instruction of the SYBR Premix Ex Taq™ kit using the cDNA as template and the specific primers of apoptosis-related gene caspase-3, anti-apoptosis gene Bcl-2 and the housekeeping gene β -actin (listed in Table 1). The relative gene expressions of caspase-3 and Bcl-2 compared with β -actin were analyzed by fold values using the Δ Ct method as reported [16]. The experiment was repeated three times, independently.

2.8. Cell cycle analysis

The cell cycle arrest of tumor cells induced by drug is associated with the therapeutic opportunities of cancer. In this paper, the cycle arrest of B16F10 cells after treating with the drug-loaded hydrogel was assayed by Fluorescence-Activated Cell Sorter (FACS). Briefly, 6-well plates were seeded with B16F10 cells (3×10^5 cells/well) and 5 μ l of the hydrogel precursor solution (DOX: 1 mg/ml, IL-2 and IFN- γ : 10 μ g/ml) were added in each well as above. After the formation of the hydrogel by incubating at 37 °C, the cells were incubated with fresh DMEM for 15 h at 37 °C. The cells were then collected, fixed with 70% ethanol, incubated by RNase A and stained by propidium iodide (PI) as the protocol of cell cycle assay kit. The FACS analysis was then carried out within 1 h.

2.9. The degradation and biocompatibility of PELG₇-PEG₄₅-PELG₇ gel *in vivo*

The degradation and biocompatibility of PELG₇-PEG₄₅-PELG₇ were tested using SD rats (male, ~200 g). The rats were anaesthetized using diethyl ether and subcutaneously injected of PELG₇-PEG₄₅-PELG₇ solution (4.0 wt%, 0.4 ml/rat). The formed gel under the skin was photographed and weighted at predetermined time intervals. Three separate tests were performed for each data point. Additionally, the inflammatory response of the skin tissue adjacent to the gel was evaluated by hematoxylin-eosin (H&E) staining as previous report.

2.10. Anti-tumor efficacy of the drug-loaded hydrogels *in vivo*

The *in vivo* anti-tumor efficacy of drug-loaded hydrogel was evaluated using a BALB/C mice (female, 6 week) model bearing B16F10 xenograft. Briefly, the B16F10 cells suspension was injected subcutaneously into the armpit of right limb of mice (0.1 ml PBS containing 1.5×10^6 cells per mice) and the tumor was then formed

Table 1
The primer sequences used for real-time PCR.

Gene	Gene ID	Forward primer	Reverse primer
β -actin	BC002409	CTGGGACGACATGGAGAAAA	AAGGAAGGCTGGAAGAGTGC
Bcl-2	NM_000633.2	ATGTGTGTGGAGAGCGTCAAC	AGAGACAGCCAGGAGAAATCAAAC
Caspase-3	NM_004346.3	ATCACAGCAAAGGAGCAGTTT	ACACCACTGTCTGTCTCAATGC

about 1 week later. The mice bearing B16F10 tumor were divided into 6 groups randomly when the volume of the tumors was about 100 mm^3 (5 mice/group, including PBS control group, hydrogel control group, DOX/IL-2/IFN- γ solution group, DOX-loaded hydrogel group, IL-2/IFN- γ co-loaded hydrogel group and DOX/IL-2/IFN- γ co-loaded hydrogel group). The treatment was then carried out by single injection of drugs or drug-loaded hydrogel beside the tumor (DOX: 1 mg/ml, IL-2 and IFN- γ : 10 $\mu\text{g}/\text{ml}$, 0.1 ml per mice, one injection). To evaluate the therapeutic efficacy and safety of the drug-loaded hydrogel, the volume of the tumor and body weight of the mice were recorded every other day. The volume of the tumor was calculated according to the formula: $V = \text{Long diameter} \times \text{Wide diameter}^2/2$, while the tumor growth inhibition (TGI) was calculated following the formula: $\text{TGI} = (\text{the average volume of PBS group} - \text{the average volume of experiment group})/\text{the average volume of PBS group} \times 100\%$.

After the experiment, the tumors were collected and the apoptosis of the tumor was analyzed by TUNEL according to the protocol of TUNEL assay kit. In addition, the apoptosis-related genes of the tumor were detected by qRT-PCR as above, and the three separate samples were tested for each point. Moreover, the pathology analysis of the tumor and the organs of the mice (hearts, lungs, livers, spleens, kidneys) were also analyzed by hematoxylin/eosin (H&E) [18].

2.11. Detection of $\text{CD3}^+/\text{CD4}^+$ T-lymphocytes, $\text{CD3}^+/\text{CD8}^+$ T-lymphocytes and NK cells of peripheral blood

The BALB/C mice bearing B16F10 tumor were divided as hydrogel group, DOX-loaded hydrogel group, IL-2/IFN- γ co-loaded hydrogel group and DOX/IL-2/IFN- γ co-loaded hydrogel group (3 mice/group) as above. Three weeks later, the peripheral blood were collected from orbital venous and added into the 1.5 ml tube pre-treated with EDTA-PBS. Then the CD3-FITC, CD4-PE and CD8-PerCP antibodies of mice were added and incubated for 25 min at 25 °C to analyze the T-lymphocytes cells. Moreover, CD3e-PE and CD49b-FITC antibodies were also added and incubated as above for the NK cell detection. After that, the erythrocyte lysate solution was added and incubated for another 15 min. After centrifugation, the supernatant was discarded and the lymphocytes were washed using PBS. The antibody-stained lymphocytes were then analyzed by FACS within 1 h. The double positive cells of CD3 and CD4 antibodies were regard as $\text{CD3}^+/\text{CD4}^+$ T-lymphocytes, double positive cells of CD3 and CD8 antibodies were regard as $\text{CD3}^+/\text{CD8}^+$ T-lymphocytes, and the double positive cells of CD3e and CD49b antibodies were regard as NK cells.

The animal experiments in this experiment were performed according with the Direction of Institution Animal Care and Use Committee of Jilin University, China.

2.12. Statistic analysis

The statistical differences of the experiments were analyzed using paired Student's-test. The difference was regard to be significant (*) if $p < 0.05$, highly significant (**) if $p < 0.01$ and extreme significant (***) if $p < 0.001$.

3. Results and discussion

3.1. The characterization of the PELG₇-PEG₄₅-PELG₇ triblock copolymer

After synthesis of the PELG₇-PEG₄₅-PELG₇ triblock copolymer via ring-opening polymerization of γ -ethyl-L-glutamate-N-carboxyanhydride (ELG-NCA) initiated by NH_2 -PEG- NH_2 , the molecular weight (Mw) and the degree of polymerization (DP) of the PELG blocks were characterized by ^1H NMR and GPC. The results showed that the Mw of the copolymer was 4200 and the total DP of two PELG blocks was 14 (Table 2 and Fig. S1). The chemical structure of the triblock copolymer was also consistent with the theoretical design as confirmed by ^1H NMR result.

3.2. Phase diagram and rheology analysis

The sol-gel phase transition temperature of thermo-sensitive hydrogels is closely associated with the hydrophilic-hydrophobic property, and is an important factor for the application as a drug deliver carrier [34]. In this paper, the sol-to-gel transition temperatures of PELG₇-PEG₄₅-PELG₇ copolymer solutions and the solutions containing drugs were tested using tube inversion method. As shown in Fig. 1a, the PELG₇-PEG₄₅-PELG₇ copolymer solutions at polymer concentrations of 3–6 wt% showed sol-to-gel phase transitions with increasing temperature. Moreover, the phase transition temperatures of the copolymer solutions decreased when the polymer concentration increased from 3 wt% to 6 wt%. In our previous study, the gelation mechanism of the PELG-PEG-PELG triblock copolymer solution has been proposed to be likely attributed to the formation of micelle aggregation network caused by both the partial dehydration of PEG chains and the change in secondary structure of the polypeptide block as temperature increased [37]. It was found that, after loading the drugs, the sol-gel phase transition temperatures also reduced slightly, which may due to the alteration of the hydrophobic-hydrophilic balance of the system. Additionally, the rheology analysis of the PELG₇-PEG₄₅-PELG₇ solutions clearly displayed the obvious increase of the storage moduli (G') with increasing temperature from 5 °C to over 20 °C, confirming the thermo-induced gel formation process (Fig. 1b). As the polymer concentration increased, the G' also was augmented. Taking the transition temperature and the G' into consideration, the 4 wt% copolymer solutions were selected in the further studies.

3.3. In vitro drug release from the drug-loaded hydrogel

The sustained drug release property of localized drug delivery

Table 2
The properties of PELG₇-PEG₄₅-PELG₇ copolymers.

Copolymer	Feed ratio of ELG-NCA/PEG	DP of PELG ^a	Mn ^a	Mn ^b	PDI ^b
PELG ₇ -PEG ₄₅ -PELG ₇	16	14	4200	4900	1.06

^a Determined by ^1H NMR.

^b Determined by GPC.

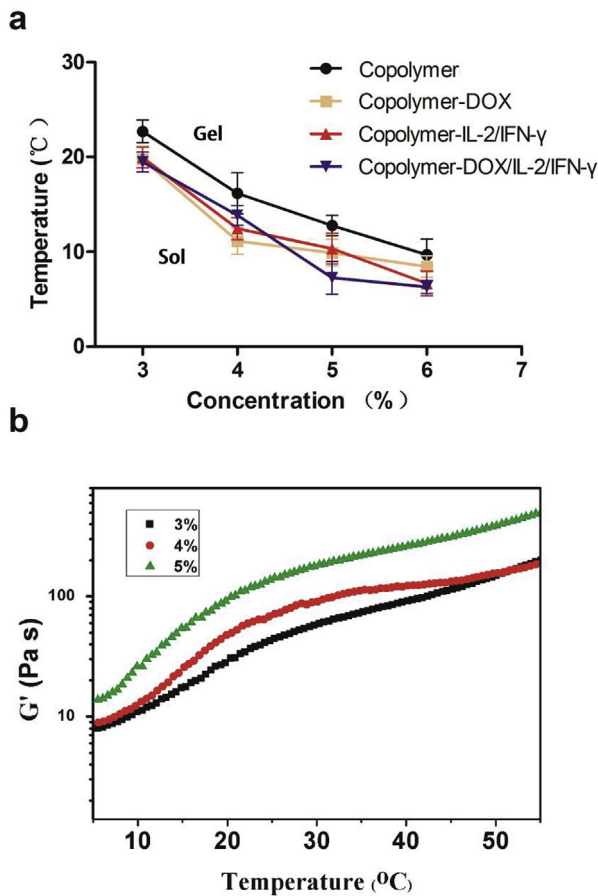


Fig. 1. Phase diagram of the PELG₇-PEG₄₅-PELG₇ triblock copolymer or drug-loaded copolymers aqueous solutions (a) and Rheology of the copolymer (b). (The concentration of DOX was 1 mg/ml and the concentrations of IL-2 and IFN- γ were both 10 μ g/ml).

system is an important fact that influences the antitumor therapeutic effects. In this study, the drug release behavior was investigated *in vitro*. To keep the biological activity of the proteins, we used the PBS containing 0.1 wt% SDS as the release medium [35]. As shown in Fig. 2, the drug release process included a short burst release phase in the first 3 days and the following sustained release term in the later 26 days, which should be due to different release

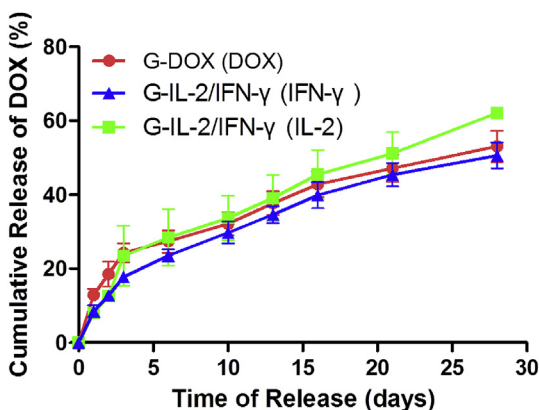


Fig. 2. The DOX, IL-2 and IFN- γ releases from drug-loaded hydrogel *in vitro*. The concentration of DOX was 1 mg/ml and the concentrations of IL-2 and IFN- γ were 10 μ g/ml in the 4% copolymers solutions before the hydrogel formation).

mechanisms. The initial burst release process may be due to diffusion of drugs while the following sustained release may be caused by the combination process of both the drug diffusion and the degradation of the hydrogel. It is noteworthy that the sustained release profiles of the chemotherapeutic drug and cytokines may contribute to long-term anti-tumor therapeutic efficiency.

3.4. *In vitro* biocompatibility of PELG₇-PEG₄₅-PELG₇

The biocompatibility of the PELG₇-PEG₄₅-PELG₇ copolymer is another key property for biomedical applications. In this paper, the biocompatibility of the PELG₇-PEG₄₅-PELG₇ copolymer was measured by MTT against B16F10 cells *in vitro*. As shown in Fig. S2, the B16F10 cells incubated with PELG₇-PEG₄₅-PELG₇ remained over 80% viable at the polymer concentrations up to 20 g/L after incubation with the copolymer for 24 h. This result indicated that PELG₇-PEG₄₅-PELG₇ presented good cytocompatibility *in vitro*.

3.5. Cytotoxicity evaluation of drugs or multi-drug co-loaded hydrogels against B16F10 cells

The cytotoxicities of the drugs and drug-loaded hydrogels were evaluated by MTT assay against B16F10 cells. The results showed that the cell viability of DOX/IL-2/IFN- γ treated group was lower than the DOX treated group and IL-2/IFN- γ treated group, indicating enhanced cytotoxicity by the combination of DOX, IL-2 and IFN- γ (Fig. S3). Moreover, drug-loaded hydrogels group exhibited lower cytotoxicities *in vitro*, compared to the free drugs group, which may be due to the slow release of drugs from the hydrogel.

3.6. Apoptosis analysis of multi-drug co-loaded hydrogels

Apoptosis is a programmed death process and plays an important role in the cell death. In this study, the apoptosis of B16F10 cells induced by the treatment with drug-loaded hydrogel was determined by FACS assay. As shown in Fig. 3a, the apoptosis cell ratio of DOX/IL-2/IFN- γ co-loaded hydrogel group was increased obviously compared with the blank hydrogel group (Gel group), DOX-loaded hydrogel group and IL-2/IFN- γ co-loaded hydrogel group. This was consistent with the cytotoxicity measurement. Moreover, the apoptosis-related gene expressions were detected by Real-time PCR. As shown in Fig. 3b, the expression of the anti-apoptosis Bcl-2 gene of the DOX/IL-2/IFN- γ co-loaded hydrogel group reduced and the expression of apoptosis gene caspase-3 increased, compared with the control groups, which was consistent with the apoptosis detection by FACS. The increased cell apoptosis may be the cause of the increased cytotoxicity of the DOX/IL-2/IFN- γ combination.

3.7. Analysis of cell cycle arrest induced by multi-drug co-loaded hydrogels

For further investigate the toxicity mechanism of the multi-drug co-loaded hydrogels, the cell cycle arrest induced by the drug loaded hydrogels was analyzed by FACS. As shown in Fig. 4, the cells were arrested at G2/S phase after DOX-loaded hydrogel treatment and at S phase after IL-2/IFN- γ co-loaded hydrogel treatment. Moreover, enhanced G2/S phase arrest was observed after treatment with DOX/IL-2/IFN- γ co-loaded hydrogel, indicating the improved tumor cell inhibition efficiency by the combination of DOX, IL-2 and IFN- γ .

3.8. Gel degradation and biocompatibility *in vivo*

Both degradation and biocompatibility are crucial properties for

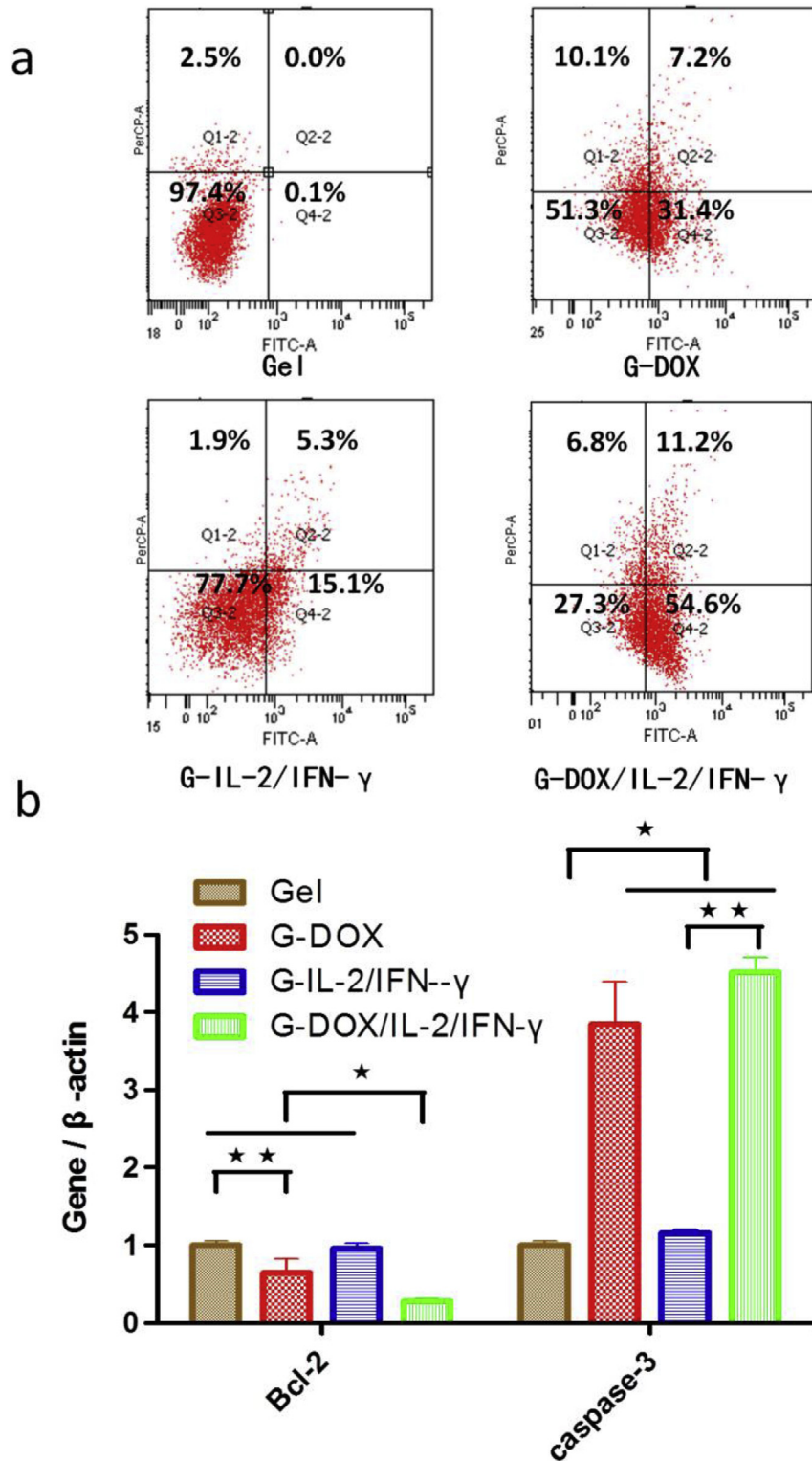


Fig. 3. The Apoptosis of B16F10 cells induced by Gel, DOX loaded hydrogel, IL-2/IFN- γ loaded hydrogel and DOX/IL-2/IFN- γ co-loaded hydrogel for 20 h detected by flow cytometry (a) and the expresses of apoptosis related genes detected by Real-time PCR (b). The lower-left (Q3-3), upper-left (Q1-3), upper-right (Q2-3) and lower-right (Q4-3) quadrants in each panel of Fig. a indicated the populations of normal, early apoptotic, late apoptotic and apoptotic necrotic cells, respectively. Data of related gene expressions in Fig. b were normalized to β -actin (* $p < 0.05$, ** $p < 0.01$).

the thermo-sensitive hydrogel when used as drug carriers *in vivo*. The degraded process of the PELG₇-PEG₄₅-PELG₇ hydrogel in the subcutaneous layer of rats was observed and the biocompatibility *in vivo* was analyzed by H&E staining of the skin around the

hydrogels every week after injection of the copolymer solution (4.0 wt%) into the rats subcutaneously. As shown in Fig. 5a and Fig. 5b, the hydrogel showed about 52.43% mass loss in the first week after injection and degraded completely 3 weeks later. The

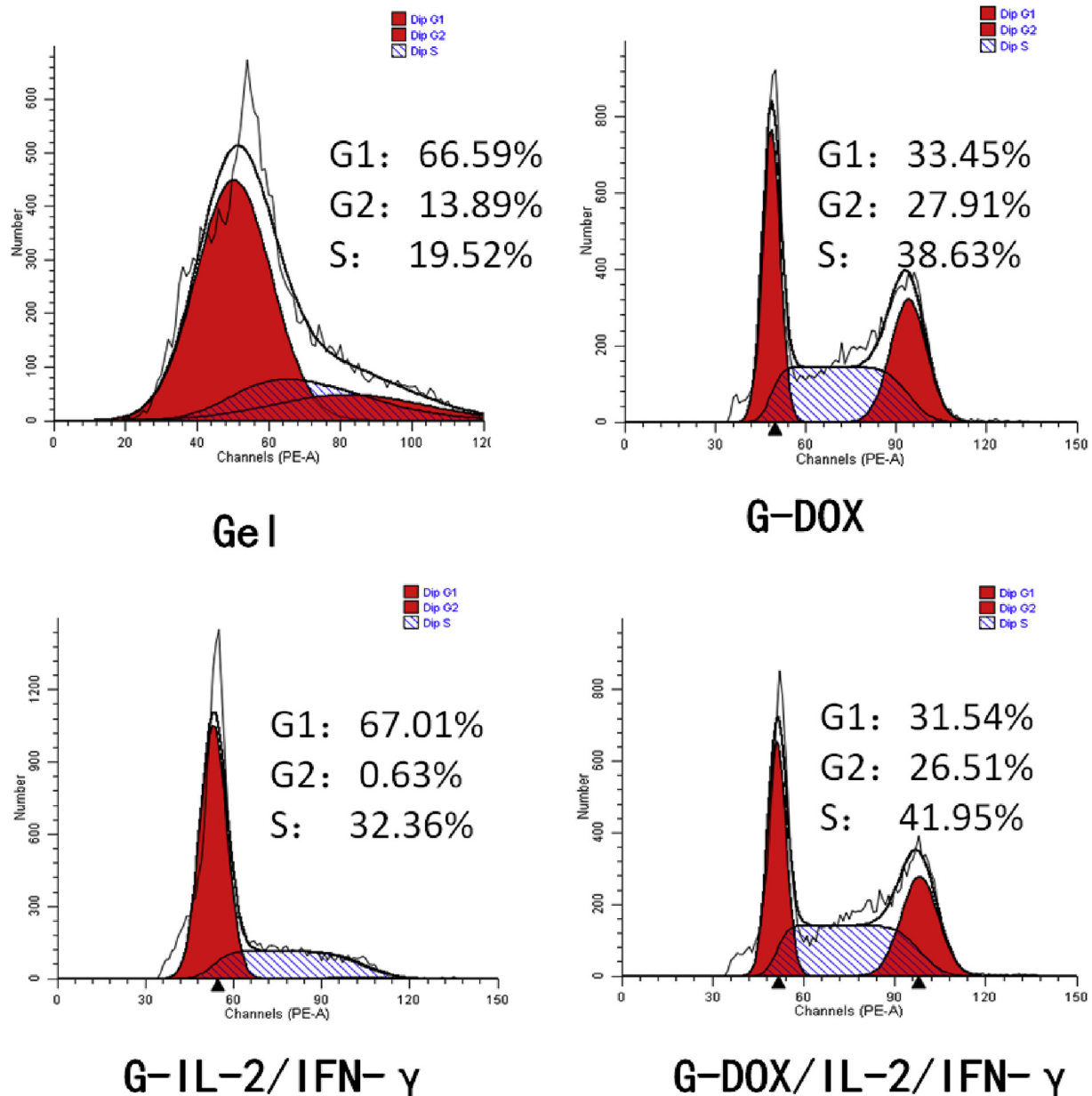


Fig. 4. Cell cycle arrest of B16F10 cells induced by Gel, DOX loaded hydrogel, IL-2/IFN- γ loaded hydrogel and DOX/IL-2/IFN- γ co-loaded hydrogel for 15 h respectively. The figure showed the G1, G2 and S proportions of each group.

degradation of polypeptide-based hydrogel may be driven by the effects of proteolytic enzymes *in vivo* [37]. The H&E staining results of the skin tissue showed no obvious necrosis, hemorrhaging, and muscle damage appeared during the degradation process except for a weak acute inflammation with slightly enhanced neutrophils near the injection site at 7 day after injection (Fig. 5c). However, the inflammation was disappeared 14 days later and the surrounding tissue returned to normal state, implying acceptable biocompatibility of the PELG₇-PEG₄₅-PELG₇ hydrogel *in vivo*.

3.9. Therapeutic efficiency of the multi-drug co-loaded hydrogel against B16F10 tumor *in vivo*

The therapeutic efficiency of the drug-loaded hydrogels against B16F10 tumor was evaluated *in vivo*. As shown in Fig. 6, the tumor of the group treated with blank hydrogel grew as fast as the PBS

group (the statistical difference of the two groups was not significant, $p > 0.05$). Notably, all the groups treated with drug-containing solutions or hydrogels showed tumor inhibition efficacy compared to the control groups (PBS treated group and blank hydrogel group). The tumor growth inhibition (TGI) of DOX/IL-2/IFN- γ co-loaded hydrogel (91.51%) was found to be greater than DOX/IL-2/IFN- γ solution group (56.08%), likely attributed to the local sustain release of the multiple drugs by the hydrogel. Moreover, the TGI of the DOX/IL-2/IFN- γ co-loaded hydrogel group was also higher than the DOX-loaded hydrogel (57.40%) and IL-2/IFN- γ co-loaded hydrogel (28.22%) (Fig. 6a), indicating markedly improved anti-tumor efficiency by the localized co-delivery of the chemotherapeutic drug and immunomodulatory cytokines. Moreover, the monitoring on the body weights of the mice showed no obvious systemic toxicity by the localized treatment (Fig. 6c).

The detection of apoptosis-related genes by qRT-PCR indicated

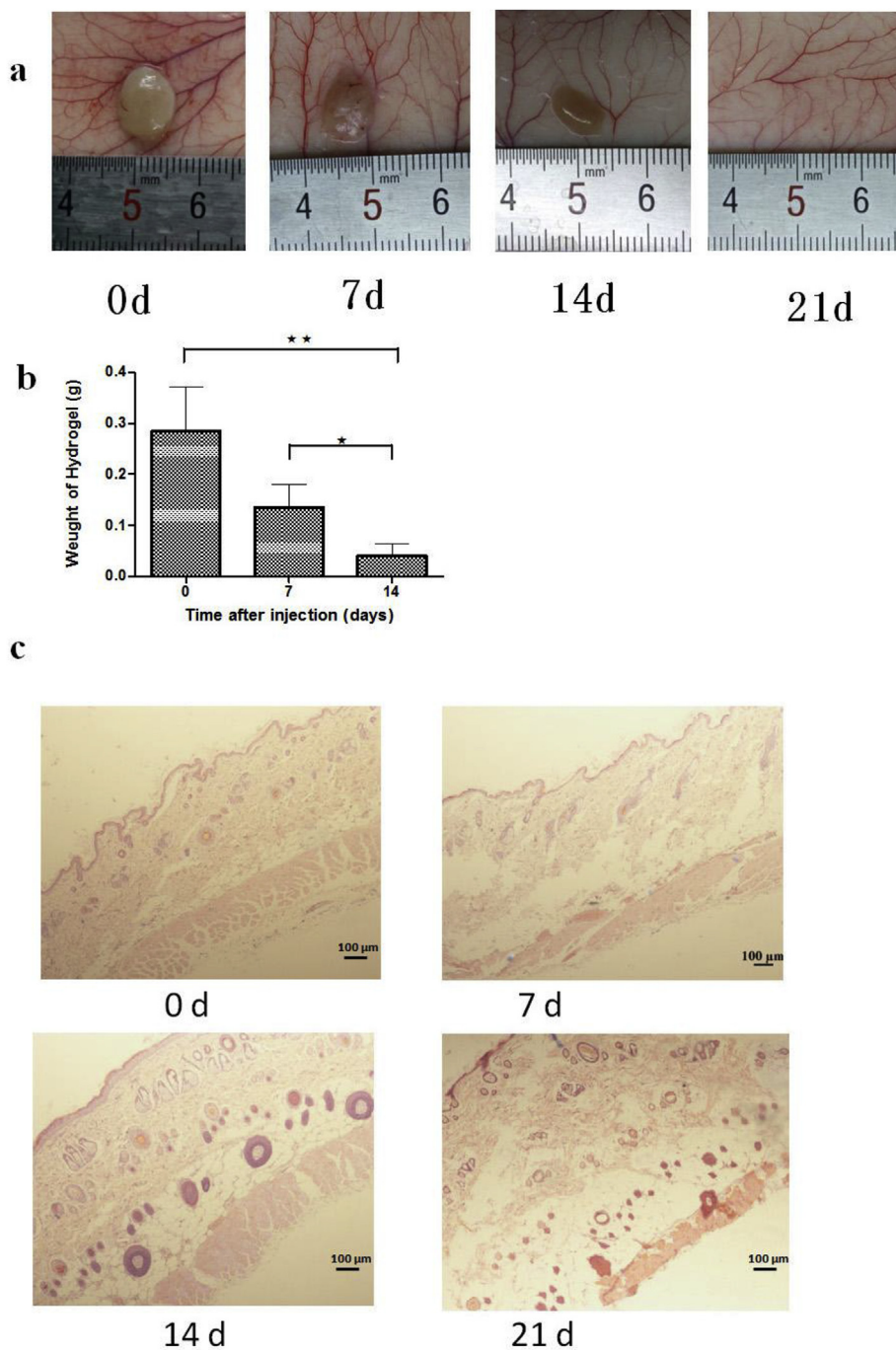


Fig. 5. The degradation and biocompatibility of the PELG₇-PEG₄₅-PELG₇: The photos of degraded hydrogel under the skin of rats (a), the weight of hydrogel (b) and the H&E results of skin around the hydrogel (c, 20 ×). The observation term was 21d till the hydrogel degraded completely (*p < 0.05, **p < 0.01).

that the expression of Bcl-2 gene was reduced and the expression of caspase-3 for the group treated with the DOX/IL-2/IFN- γ co-loaded hydrogel was increased compared with the control groups, confirming the enhanced apoptosis induced by the treatment with sustained release of DOX, IL-2 and IFN- γ (Fig. 6d). The apoptosis of the tumor was analyzed by TUNEL assay and the results showed that the tumor of the group treated with DOX/IL-2/IFN- γ co-loaded hydrogel exhibited the highest apoptosis (Fig. 7). The H.E staining results also showed the tumor cells of the group treated with DOX/IL-2/IFN- γ co-loaded hydrogel exhibited most pathology, such as karyolysis, pyknosis and karyorrhexis, which was consistent with the apoptosis results. Overall, the results indicated that the

enhanced inhibition of tumor growth by the DOX/IL-2/IFN- γ co-loaded hydrogel was caused by the apoptosis of tumor cells.

The H&E analysis of the major organs of mice including hearts, lungs, livers, spleens, kidneys showed there was no obvious pathology damage (Fig. S4). This was consistent with no obvious reduction in the body weight of the mice, which suggested no significant systemic toxicity of the localized delivery systems.

3.10. The immune mechanism induced by combined therapy

To investigate the immune mechanism induced by the DOX/IL-2/IFN- γ co-loaded hydrogel, the CD3⁺/CD4⁺ and CD3⁺/CD8⁺ T-

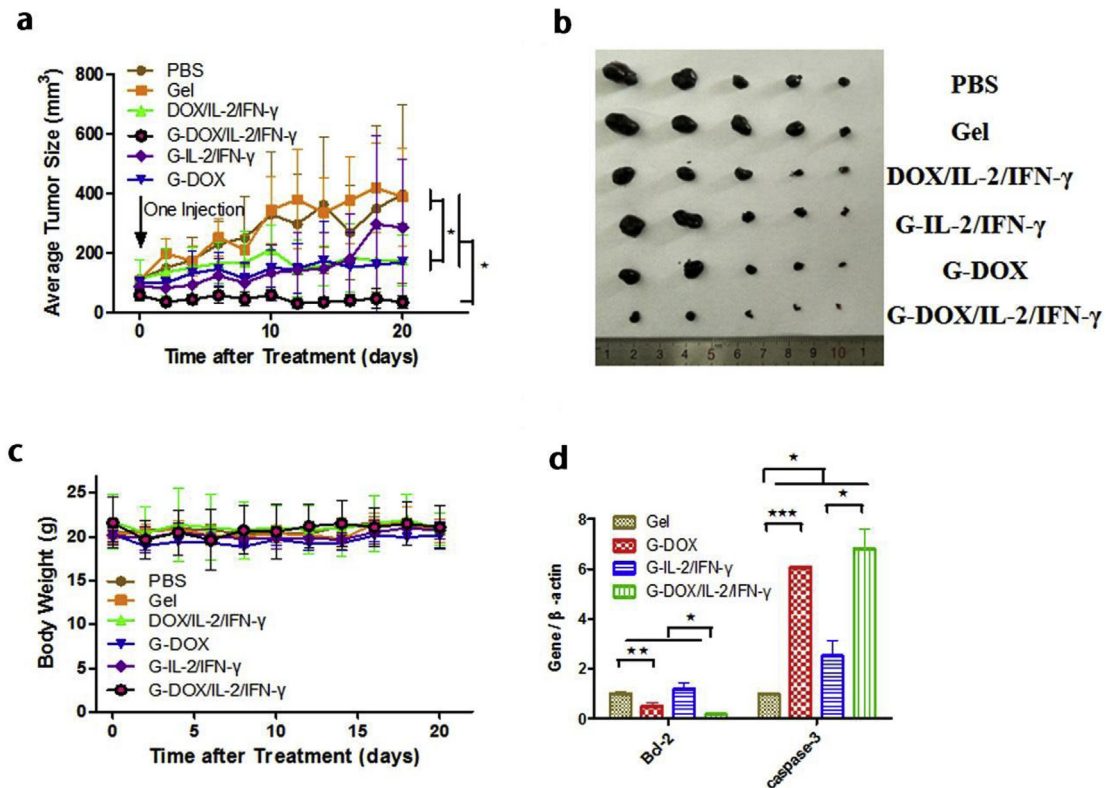


Fig. 6. *In vivo* B16F10 tumor treated effects of free drugs and drug-loaded hydrogels: Volume of tumors (a), the weights of tumors(b), the photos of tumors(c) and the body weight change of mice during treatments(d), (* $p < 0.05$, ** $p < 0.01$, *** $p < 0.001$).

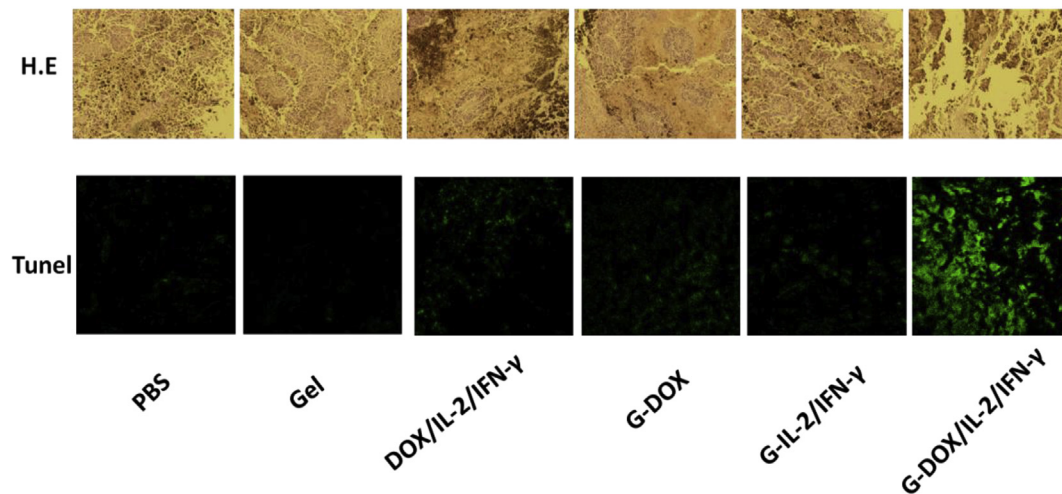


Fig. 7. The H&E staining and TUNEL analyses of B16F10 tumor (Nuclei of the cells were stained blue, and cytoplasm were stained as red in H&E staining. Green fluorescence indicated apoptotic cells of tumor in TUNEL analysis).

lymphocytes of peripheral blood were detected by FACS. As shown in Fig. 8, it was found that both the numbers of $CD3^+/CD4^+$ T-lymphocytes and $CD3^+/CD8^+$ T-lymphocytes increased significantly after the treatment with the DOX/IL-2/IFN- γ co-loaded hydrogel, compared to the blank hydrogel group and the group treated with the hydrogel containing only DOX or cytokines (IL-2/IFN- γ). Though the number of NK cells also increased in the group treated with DOX/IL-2/IFN- γ co-loaded hydrogel, no significant difference was observed. As we known, both $CD3^+/CD8^+$ T-lymphocytes and $CD3^+/CD4^+$ T-lymphocytes are important

immunotherapeutic modulators in the control of tumor growth. The $CD3^+/CD8^+$ T-lymphocytes (cytotoxic T-lymphocytes) usually displayed cytotoxic functions by migrating to sites of tumor and kill tumor cells directly, while $CD3^+/CD4^+$ T-lymphocytes (helper T-lymphocytes) provided help to innate immune responses, B cells as well as $CD8^+$ T cells, to kill tumor cells. Our previous study showed that DOX/IL-2/IFN- γ exhibited synergistic anti-tumor effects by inducing the apoptosis through regulating the genes of Janus kinase, JAK/STAT and mitochondrial signal pathways [19]. The results of this study showed that the localized, co-delivery of DOX, IL-2 and

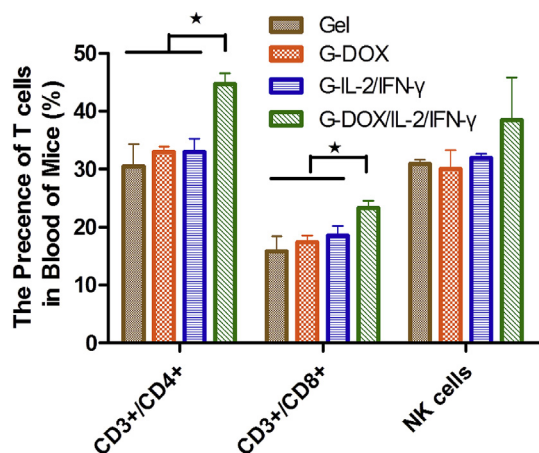


Fig. 8. Detection of CD3⁺/CD4⁺ T-lymphocytes, CD3⁺/CD8⁺ T-lymphocytes and NK cells of peripheral blood of the mice (*p < 0.05).

IFN-γ could also cause enhanced immune responses by promoting the proliferation of the immune cells *in vivo*, including CD3⁺/CD4⁺ T-lymphocytes and CD3⁺/CD8⁺ T-lymphocytes.

4. Conclusions

In this paper, a strategy of localized, co-delivery of DOX, IL-2 and IFN-γ based on the biodegradable and biocompatible PELG7-PEG45-PELG7 hydrogel was developed for the local therapy of melanoma. The drug release process included a short term of initial burst release and a following long-term sustained release of the three agents. The polypeptide hydrogel was found to last 3 weeks in the subcutaneous layer of rats with good biocompatibility *in vivo*. The DOX/IL-2/IFN-γ co-loaded hydrogel displayed enhanced anti-tumor effect on B16F10 cells *in vitro* by improving the cytotoxicity, increasing the ratio of cell apoptosis and cell cycle of G2/S phase arrest. Additionally, the strategy by the localized, co-delivery of DOX, IL-2 and IFN-γ presented the highest tumor inhibition efficacy in the mice model bearing B16F10 xenograft, without obvious systemic side effects. The improved anti-tumor efficacy by the combination of DOX, IL-2 and IFN-γ was believed to be related to the increased inducement of the apoptosis and promoting the proliferation of immune cells including CD3⁺/CD4⁺ T-lymphocytes and CD3⁺/CD8⁺ T-lymphocytes. Based on these results, the localized, co-delivery of DOX/IL-2/IFN-γ based on the biodegradable and biocompatible polypeptide hydrogel may serve as a promising platform for efficient treatment of cancers such as melanoma.

Conflict of interest statement

The authors declare no conflict of interests.

Acknowledgments

The financial support from the National Natural Science Foundation of China (No. 51403202, 51622307, 51390484, 51520105004) are gratefully thanked.

Appendix A. Supplementary data

Supplementary data related to this article can be found at <http://dx.doi.org/10.1016/j.bioactmat.2017.08.003>.

References

- [1] H. Tsao, Management of cutaneous melanoma, *N. Engl. J. Med.* 351 (2004) 998–1012.
- [2] S.S. Agarwala, Current systemic therapy for metastatic melanoma, *Expert Rev. Anticancer Ther.* 9 (2009) 587–595.
- [3] A. Hauschild, C. Garbe, Immunotherapy: combined immunotherapy—a new standard in metastatic melanoma? *Nat. Rev. Clin. Oncol.* 12 (2015) 439–440.
- [4] F.S. Hodi, S.J. O'Day, D.F. McDermott, R.W. Weber, J.A. Sosman, J.B. Haanen, et al., Improved survival with ipilimumab in patients with metastatic melanoma, *N. Engl. J. Med.* 363 (2010) 711–723.
- [5] M. Dougan, G. Dranoff, Immune therapy for cancer, *Annu. Rev. Immunol.* 27 (2009) 83–117.
- [6] A. Nicolini, A. Carpi, G. Rossi, Cytokines in breast cancer, *Cytokine Growth F. R.* 17 (2006) 325–337.
- [7] D. Lienard, P. Ewalenko, J.J. Delmotte, N. Renard, F.J. Lejeune, High-dose recombinant tumor necrosis factor alpha in combination with interferon gamma and melphalan in isolation perfusion of the limbs for melanoma and sarcoma, *J. Clin. Oncol.* 10 (1992) 52–60.
- [8] N. Sakamoto, T. Ishikawa, S. Kokura, T. Okayama, K. Oka, M. Ideno, et al., Phase I clinical trial of autologous NK cell therapy using novel expansion method in patients with advanced digestive cancer, *J. Transl. Med.* 13 (2015).
- [9] S.A. Rosenberg, M.T. Lotze, J.C. Yang, W.M. Linehan, C. Seipp, S. Calabro, et al., Combination therapy with interleukin-2 and alpha-interferon for the treatment of patients with advanced cancer, *J. Clin. Oncol.* 7 (1989) 1863–1874.
- [10] S. Nair, D. Boczkowski, B. Moeller, M. Dewhurst, J. Vieweg, E. Gilboa, Synergy between tumor immunotherapy and antiangiogenic therapy, *Blood* 102 (2003) 964–971.
- [11] J. Larkin, F.S. Hodi, J.D. Wolchok, Combined nivolumab and ipilimumab or monotherapy in untreated melanoma reply, *N. Engl. J. Med.* 373 (2015) 1270–1271.
- [12] H. Cho, G.S. Kwon, Thermosensitive poly-(D,L-lactide-co-glycolide)-block-poly(ethylene glycol)-block-poly-(D, L-lactide-co-glycolide) hydrogels for multi-drug delivery, *J. Drug Target.* 22 (2014) 669–677.
- [13] T. Li, M. Zhang, J. Wang, T. Wang, Y. Yao, X. Zhang, et al., Thermosensitive hydrogel Co-loaded with gold nanoparticles and doxorubicin for effective chemoradiotherapy, *Aaps J.* 18 (2016) 146–155.
- [14] A. GhavamiNejad, M. SamariKhalaj, L.E. Aguilar, C.H. Park, C.S. Kim, pH/NIR light-controlled multidrug release via a mussel-inspired nanocomposite hydrogel for chemo-photothermal cancer therapy, *Sci. Rep.* 6 (2016).
- [15] A. Ribas, F.S. Hodi, M. Callahan, C. Konto, J. Wolchok, Hepatotoxicity with combination of vemurafenib and ipilimumab, *N. Engl. J. Med.* 368 (2013) 1365–1366.
- [16] H.A. Meng, M. Liang, T.A. Xia, Z.X. Li, Z.X. Ji, J.I. Zink, et al., Engineered design of mesoporous silica nanoparticles to deliver doxorubicin and P-Glycoprotein siRNA to overcome drug resistance in a cancer cell line, *ACS Nano* 4 (2010) 4539–4550.
- [17] E.F. McClay, M.J. Mastrangelo, D. Berd, R.E. Bellet, Effective combination chemo/hormonal therapy for malignant melanoma: experience with three consecutive trials, *Int. J. Cancer* 50 (1992) 553–556.
- [18] X.L. Wu, Y.D. Wu, H.B. Ye, S.J. Yu, C.L. He, X.S. Chen, Interleukin-15 and cisplatin co-encapsulated thermosensitive polypeptide hydrogels for combined immuno-chemotherapy, *J. Control. Release* 255 (2017) 81–93.
- [19] X.L. Wu, C.L. He, Y.D. Wu, X.S. Chen, J.J. Cheng, Nanogel-incorporated physical and chemical hybrid gels for highly effective chemo-protein combination therapy, *Adv. Funct. Mater.* 25 (2015) 6744–6755.
- [20] W. Zhu, Y.L. Li, L.X. Liu, Y.M. Chen, F. Xi, Supramolecular hydrogels as a universal scaffold for stepwise delivering Dox and Dox/cisplatin loaded block copolymer micelles, *Int. J. Pharm.* 437 (2012) 11–19.
- [21] S. Barua, S. Mitravotri, Synergistic targeting of cell membrane, cytoplasm, and nucleus of cancer cells using rod-shaped nanoparticles, *ACS Nano* 7 (2013) 9558–9570.
- [22] S. Eikawa, M. Nishida, S. Mizukami, C. Yamazaki, E. Nakayama, H. Udono, Immune-mediated antitumor effect by type 2 diabetes drug, metformin, *Proc. Natl. Acad. Sci. U. S. A.* 112 (2015) 1809–1814.
- [23] H. Tsukamoto, S. Senju, K. Matsumura, S.L. Swain, Y. Nishimura, IL-6-mediated environmental conditioning of defective Th1 differentiation dampens anti-tumour immune responses in old age, *Nat. Commun.* 6 (2015).
- [24] J. Park, S.H. Wrzesinski, E. Stern, M. Look, J. Criscione, R. Ragheb, et al., Combination delivery of TGF-beta inhibitor and IL-2 by nanoscale liposomal polymeric gels enhances tumour immunotherapy, *Nat. Mater.* 11 (2012) 895–905.
- [25] S.A. Rosenberg, J.C. Yang, D.J. Schwartzentruber, P. Hwu, F.M. Marincola, S.L. Topalian, et al., Prospective randomized trial of the treatment of patients with metastatic melanoma using chemotherapy with cisplatin, dacarbazine, and tamoxifen alone or in combination with interleukin-2 and interferon alfa-2b, *J. Clin. Oncol.* 17 (1999) 968–975.
- [26] A.J. Lumsden, J.P. Codde, B.N. Gray, P.H. van der Meide, Improved efficacy of doxorubicin by simultaneous treatment with interferon-gamma and interleukin-2, *In Vivo* 6 (1992) 553–558.
- [27] S.S. Legha, S. Ring, O. Eton, A. Bedikian, A.C. Buzaid, C. Plager, et al., Development of a biochemotherapy regimen with concurrent administration of cisplatin, vinblastine, dacarbazine, interferon alfa, and interleukin-2 for patients with metastatic melanoma, *J. Clin. Oncol.* 16 (1998) 1752–1759.

- [28] S.A. Del Prete, L.H. Maurer, J. O'Donnell, R.J. Forcier, P. LeMarbre, Combination chemotherapy with cisplatin, carmustine, dacarbazine, and tamoxifen in metastatic melanoma, *Cancer Treat. Rep.* 68 (1984) 1403–1405.
- [29] N. Yoon, M.S. Park, G.C. Peltier, R.H. Lee, Pre-activated human mesenchymal stromal cells in combination with doxorubicin synergistically enhance tumor-suppressive activity in mice, *Cytotherapy* 17 (2015) 1332–1341.
- [30] Z. Guo, H.L. Wang, F.D. Meng, J. Li, S.L. Zhang, Combined Trabectedin and anti-PD1 antibody produces a synergistic antitumor effect in a murine model of ovarian cancer, *J. Transl. Med.* 13 (2015).
- [31] U. Keilholz, C.J.A. Punt, M. Gore, W. Kruit, P. Patel, D. Lienard, et al., Dacarbazine, cisplatin, and interferon- α -2b with or without interleukin-2 in metastatic melanoma: a randomized phase III trial (18951) of the European Organisation for Research and Treatment of Cancer Melanoma Group, *J. Clin. Oncol.* 23 (2005) 6747–6755.
- [32] D. Khayat, C. Borel, J.M. Tourani, A. Benhammouda, E. Antoine, O. Rixe, et al., Sequential chemoimmunotherapy with cisplatin, interleukin-2, and interferon α -2a for metastatic melanoma, *J. Clin. Oncol.* 11 (1993) 2173–2180.
- [33] E. Oh, J.-E. Oh, J. Hong, Y. Chung, Y. Lee, K.D. Park, et al., Optimized biodegradable polymeric reservoir-mediated local and sustained co-delivery of dendritic cells and oncolytic adenovirus co-expressing IL-12 and GM-CSF for cancer immunotherapy, *J. Control. Release* (2017), <http://dx.doi.org/10.1016/j.jconrel.2017.03.028>.
- [34] N. Doshi, S. Mitragotri, Designer biomaterials for nanomedicine, *Adv. Funct. Mater* 19 (2009) 3843–3854.
- [35] M. Qiao, D. Chen, T. Hao, X. Zhao, H. Hu, X. Ma, Injectable thermosensitive PLGA-PEG-PLGA triblock copolymers-based hydrogels as carriers for interleukin-2, *Pharmazie* 63 (2008) 27–30.
- [36] C.L. Peng, Y.H. Shih, K.S. Liang, P.F. Chiang, C.H. Yeh, I.C. Tang, et al., Development of in situ forming thermosensitive hydrogel for radiotherapy combined with chemotherapy in a mouse model of hepatocellular carcinoma, *Mol. Pharm.* 10 (2013) 1854–1864.
- [37] Y.L. Cheng, C.L. He, J.X. Ding, C.S. Xiao, X.L. Zhuang, X.S. Chen, Thermosensitive hydrogels based on polypeptides for localized and sustained delivery of anticancer drugs, *Biomaterials* 34 (2013) 10338–10347.